Canadian Journal of Forest Research

OPEN ACCESS | Research Article

Melampsora larici-populina homologous effectors Mlp72983 and Mlp52166 display cell-type specific accumulation in *Arabidopsis* and *Populus*

Snehi Gazal[a], Karen Cristine Gonçalves dos Santos[a], Mélodie B. Plourde[a], Caroline Levasseur[b], Armand Séguin[b], Philippe Tanguay[b], Benjamin Petre[c], and Hugo Germain[a]

[a]Department of Chemistry, Biochemistry and Physics, Université du Québec à Trois-Rivières, Trois-Rivières, QC G9A 5H7, Canada; [b]Canadian Forest Service, Laurentian Forestry Centre, Natural Resources Canada, Sainte-Foy, QC G1V 4C7, Canada; [c]Université de Lorraine, INRAE, IAM, F-54000 Nancy, France

Corresponding author: **Hugo Germain** (email: hugo.germain@uqtr.ca)

Abstract

Plants interact with microorganisms that can cause diseases and reduce crop productivity. The fungal pathogen *Melampsora larici-populina* (*Mlp*) causes the leaf rust disease of poplar trees by secreting proteins, termed effectors, into host tissues to promote pathogenesis. In this study, we functionally characterized two homologous *Mlp* candidate secreted effector proteins (CSEPs), Mlp72983 and Mlp52166. Confocal microscopy experiments revealed that Mlp72983 has cell type-specific differential localization. It accumulates in the guard cells' chloroplast of the epidermis and in the nucleus of the spongy mesophyll of *Arabidopsis thaliana* and *Populus alba* x *Populus tremula*. Mlp52166 has a nucleocytosolic accumulation in the epidermal layer and has nuclear localization in the mesophyll layer of the two species. Transcriptomic experiments showed that Mlp72983 and Mlp52166 deregulate plant genes, when constitutively expressed in either *Arabidopsis* or poplar. The two CSEPs deregulate genes that encode histones, hydroxysteroid dehydrogenases, and multidrug and toxic compound extrusion proteins, with roles in DNA repair, methylation, and xenobiotic detoxification. Inoculation assays showed that CSEPs overexpression in poplar transgenics did not enhance susceptibility to rust infection. Despite being closely related in sequence identity, Mlp72983 and Mlp52166 have cell type-specific subcellular localization and deregulate mostly unique sets of plant genes.

Key words: Pucciniales, epidermis layer, nucleus, subcellular localization, gene deregulation

Introduction

Rust fungi (Pucciniales order) are one of the largest and most complex group of plant pathogens, causing significant losses to crops and bioresources (Dean et al. 2012). Members of this order can collectively infect a wide range of plants, ranging from gymnosperms to angiosperms. Despite being important pathogens, technical barriers, such as the lack of transformation capacity and obligation to work with living hosts, impair investigations of the biology of rust fungi (Petre and Duplessis 2022). However, in the recent decades, the sequencing of the first genomes of Pucciniales allowed functional genomics studies and fast-forwarded molecular investigations (Duplessis et al. 2011). Molecular biologists have relied on heterologous systems (since rust fungi do not infect model plants) to elucidate the pathogenicity mechanism and interaction between fungi and host plants (Lorrain et al. 2018*a*).

Melampsora larici-populina (*Mlp*) requires two phylogenetically unrelated hosts, larch and poplar, to complete its life cycle (Duplessis et al. 2009; Frey et al. 2011). *Mlp* infection plagues a variety of poplar cultivars, and high-density monoclonal cultivation has led to genetic resistances breakdown (Pinon and Frey 2005; Xhaard et al. 2011; Persoons et al. 2017). To infect poplar and larch, *Mlp* deploys putative effectors within host tissues (Hacquard et al. 2010; Joly et al. 2010). A study by Duplessis et al. (2011) revealed that the poplar rust genome encodes approximately 1184 candidate secreted effector proteins (CSEPs). These candidate secreted effectors proteins were categorized into protein families based on sequence similarity (Hacquard et al. 2012; Saunders et al. 2012). Understanding the molecular dialogue between *Mlp* and its hosts is crucial to uncovering its pathogenicity mechanism and the plant's susceptibility mechanisms.

Figuring out the role of effectors during the infection process implies, as a first step, to identify the site of accumulation of these proteins in the plant cell (Alfano 2009). A previous study on *Mlp* CSEPs by Germain et al. (2018) showed that most (11/14) localize to the nucleus and cytosol, whereas three accumulated at specific cellular compartments in *Arabidopsis thaliana*. Similarly, Mlp124478 was shown to accumulate in the nucleus and nucleolus of *A. thaliana* (Ahmed et al. 2018). Interestingly, several studies using the heterologous

system *Nicotiana benthamiana* have reported the localization of CSEPs to the chloroplasts (Petre et al. 2015; Petre et al. 2016; Andac et al. 2020). In recent studies, chloroplast-targeting fungal effectors were shown to enhance plant susceptibility to pathogens and play novel roles during pathogenesis (Xu et al. 2019; Andac et al. 2020).

Plants are composed of tissues, organs, and cell types not all equally affected by effectors (Henry et al. 2017). It has been demonstrated that *Pseudomonas syringae* can secrete AvrB and AvrPto unequally in diverse cell types and in a temporally regulated manner (Henry et al. 2017). Coherent with these findings, it also appears that the plant itself can respond to aggressors with a cell type-specific immune response (Delannoy et al. 2023; Tang et al. 2023). This dual heterogeneity, of the pathogen effector space–time modulation and the plant's uneven immunity complexifies our understanding of the plant–pathogen molecular dialog. Moreover, the widespread use of transient expression in heterologous systems such as *N. benthamiana* potentially hides some of that dynamic.

Mlp72983 and Mlp52166 belong to the small-secreted proteins (SSP) family Mlp7: they are the two closest members and share 76.9% identity in amino acid sequence (Letanneur et al. 2024). In addition, transcriptomic analysis of *Mlp* during infection of both hosts (larch and poplar) showed that these homologous CSEPs have contrasting host expressions, where Mlp72983 is highly expressed during larch infection (62.3 times more) and Mlp52166 expression predominates during poplar infection (16.2 times more) (Lorrain et al. 2018*b*). Moreover, Mlp72983 overexpression in *A. thaliana* deregulates over 700 genes, including genes involved in plant immunity (Dos Santos et al. 2021). In addition, our laboratory recently showed that both candidate effectors can induce stromule formation and that Mlp52166 does so partially dependently on EDS1, while Mlp72983 uses NRG1 (Letanneur et al. 2024). In this study, we have assessed the *in planta* activity of Mlp72983 and Mlp52166 using *Arabidopsis* and poplar transgenics. In epidermal cells, we observed a cell type-specific accumulation of Mlp72983 in the chloroplasts of guard cells and in the nucleus of spongy mesophyll cells, while Mlp52166 showed nucleocytosolic accumulation in pavement cells and nuclear accumulation in spongy mesophyll cells in both species. Transcriptomic analyses revealed that transgenics expressing these CSEPs have several hundreds of deregulated genes, including a few commonly deregulated genes. Therefore, our study reveals that similar *Mlp* CSEPs can have different cell type-specific accumulation *in planta* and modulate the expression of unique gene sets.

Materials and methods

Plasmid construction

Mlp candidate effector sequences were obtained from JGI MycoCosm (genome JGI Mellp version 2.0 (Duplessis et al. 2011)). *CaMV35S*::CSEP-*GFP* constructs were the same as described in Letanneur et al. (2024); primers are mentioned in Table S1. The constructs were sequenced before transformation into *Agrobacterium tumefaciens*. The nucleoid marker SWIB-RFP construct was used as described in Letanneur et al. (2024)

Growth condition of bacterial material

Escherichia coli DH5α cells were grown in Luria-Bertani media at 37 °C with spectinomycin (25 $\mu g\,mL^{-1}$). *Agrobacterium tumefaciens* strain GV3101 (pMP90) was grown in yeast extract peptone medium at 28 °C with 50 $\mu g\,mL^{-1}$ spectinomycin, 25 $\mu g\,mL^{-1}$ gentamycin, and 100 $\mu g\,mL^{-1}$ rifampicin.

Production of *A. thaliana* transgenics

Arabidopsis thaliana Col-0 seeds were stratified for 48 h at 4 °C, then plants were grown in soil (Agromix) in a growth chamber under 16 h:8 h light:dark conditions at 23 °C and 60% relative humidity. A slightly modified floral dipping technique was used to transform the plants with *A. tumefaciens* strain GV3101 (pMP90) to develop *Arabidopsis* transgenics (Mireault et al. 2014). Single insertion homozygous transgenics were selected using Mendelian segregation of the Basta resistance (15 mg L^{-1}) in T1 and T2 generations. Two positive independent *Arabidopsis* transgenic lines expressing Mlp52166-GFP (AT2_1_521 and AT_11_521) were selected upon observation of GFP fluorescence. Mlp72983-GFP (AT2_2_729 and AT2_14_729) were obtained from Germain et al. (2018). The four *Arabidopsis* transgenic lines expressing the *Mlp* candidate effectors displayed normal morphology, and each construct, regardless of the line, displayed identical cellular localization of the fluorescent protein; therefore, confocal images are shown for only one line per construct in each plant species. For both subcellular localization assay and transcriptomics, Col-0 expressing GFP (Col_0_GFP) was used as control (Germain et al. 2018).

Measurements of Photosystem II activity

We measured the Photosystem II (PSII) activity of the stable *Arabidopsis* transgenics expressing Mlp72983. Three cauline leaves per transgenic lines (AT2_2_Mlp729 & AT2_14_729) of *Arabidopsis* were kept in the dark for an hour, the minimal level (F_o) and then the maximum fluorescence level (F_m) was measured followed by 20 min of light exposure. After photosynthesis is fully induced, the measurement was done at 830 nm using PAM-101 (Walz) and an emitter detector pair. The interval between measurement points was 5 min upon switching the light on and off with an electronic shutter. Data acquisition system PDA-100 PAM was used to record the change in light absorption. The experiment was repeated three times

Production of poplar transgenics

To produce stable poplar transgenics, the hybrid *Populus alba* x *P. tremula* (INRA clone 717-1B4) was used. Poplar transformation was done using internode co-cultivation protocol (Leple et al. 1992), using cefotaxime (300 $mg\,L^{-1}$) as modified by Vigneault et al. (2007). The coding sequence of *Mlp* candidate effectors and poplar expressing GFP (control) were cloned into the same vector pK7FWG2 and transformed into *A. tumefaciens* strain GV3101 (pMP90). Transgenic poplars were selected on ½ MS rooting medium

supplemented with 15 mg L^{-1} of Basta (Table S2). Positive transgenic lines expressing *Mlp* CSEP-GFP were selected through confocal microscopy. Two positive poplar transgenic lines per candidate effector protein (Mlp72983: P1_LINE1_Mlp72983 and P1_LINE3_Mlp72983; Mlp52166: P1_LINE4_Mlp52166 and P1_LINE8_Mlp52166) were used for further experiments.

Image acquisition by confocal microscopy

Laser scanning confocal microscopy images were acquired using a Leica TCS SP8 (Leica Microsystems) equipped with an oil immersion objective HC PL APO CS2 40X/1.30. To stain the nuclei, leaf discs were vacuum infiltrated in water containing DAPI (10 μg mL^{-1}) for 10 min at room temperature before observation. The DAPI, GFP and mCherry fluorophores were excited in sequential mode at 405, 488, and 552 nm, respectively, and their fluorescence emission was acquired at 444–477 nm for DAPI, 500–525 nm for GFP, and 571–606 nm for mCherry. Observation of localization was done in three independent repetitions and post-acquisition image processing was performed with the software LAS-AF Lite (Version 4.0.0.11706).

RNA extraction and transcriptomic analysis

Total RNA was isolated from leaves of *Arabidopsis* and poplar with five replicates per transgenic line using RNAeasy Plant Mini Kit (Qiagen, Inc.) following manufacturer's specifications, with on column DNase treatment. Quality was assessed using Bioanalyzer 2100 (Agilent), then RNA libraries were prepared with polyA-enriched stranded system. Sequencing was performed with Illumina Novaseq PE100 at Genome Quebec Center of McGill University, QC, Canada.

The parameters used in the analysis are deposited in GitHub (https://github.com/SnehiG/Snehi_paper_2024/tree/patch-1/scripts). Raw read quality control, including adapter trimming and filtering of low-quality reads was done with fastp 0.23.4 (Chen et al. 2018; Abdollahi et al. 2021; Chen 2023). Reads were aligned to *A. thaliana* TAIR10 and *Populus trichocharpa* Pop_tri_v4 reference genomes, retrieved from *EnsemblPlants* (https://plants.ensembl.org/index.html), using the software STAR version 2.7.9.a (Durinck et al. 2009). Subsequent analyses were done using R v4.3.1 and Bioconductor v3.17 (Durinck et al. 2009). Read counting was done with the packages Rsamtools v2.160 (Morgan et al. 2017), GenomicAlignments, and GenomicFeatures (Lawrence et al. 2013). Mapping summary is provided in Fig. S1. Differential expression analysis was done with DESeq2 v1.42.0 (Love et al. 2014). For this, genes with TPM values lower than the mean threshold of expression across the samples (calculated with *DAFS* (George and Chang 2014)) were filtered out. Then, normalization factors were calculated on the top 0.5% of genes with the lowest coefficient of variation in expression level, selected with the CustomSelection v1.1 package (Dos Santos et al. 2020). We analyzed the variation between the replicates of the transgenic lines of each species with principal component analysis (PCA), with the functions *rlog* and *plotPCA* from DESeq2 v1.42.0 (Love et al. 2014). The PCA analysis revealed that Mlp72983 poplar transgenic line P1_LINE1_Mlp729 was very different compared to the other samples, shown in Fig. S2 and therefore removed for gene ontology (GO) term enrichment analysis. When comparing CSEP::GFP expressing lines with their corresponding controls (Col_0_GFP, Poplar_GFP), we considered as deregulated genes those with $\log_2$ fold change ≥ 2 and adjusted p value < 0.01. Subsequently, for each CSEP and plant species, we maintained only the genes deregulated in both transgenic lines. GO Term enrichment was calculated with the function *enricher*, with Benjamini–Hochberg p value-correction, and *simplify*, using Wang similarity measure and cut-off of 0.3, from ClusterProfiler v4.10.0 (Yu et al. 2012). Only terms with adjusted p value ≤ 0.05 and more than 2 genes were considered as enriched in each gene sets. Networks of enriched terms were plotted using the packages org.At.tair.db (Carlson 2019), GoSemSim v2.28.0 (Yu et al. 2010; Yu 2020), igraph v1.6.0 (Csardi and Nepusz 2006; Csárdi et al. 2023), ggraph 2.1.0 (Pedersen 2020), ggrepel 0.9.5 (Slowikowski 2024), and scatterpie v0.2.1. Venn diagrams were created with the package ggVennDiagram v1.5.0.

Western blot

Between 100 and 200 mg of flash-frozen poplar leaf tissue was heated at 95 °C for 10 min in 1× Laemmli buffer. After a quick centrifugation, proteins were separated on a 12% acrylamide gel, then transferred to a Trans-Blot Turbo RTA nitrocellulose membrane (Bio-Rad). GFP-tagged proteins were revealed with a 1/1000 dilution of an HRP-coupled anti-GFP antibody (sc-9996 from Santa Cruz Biotechnology) using chemiluminescence. Coomassie staining of a parallel gel was used as a loading control.

Inoculation of poplar transgenics with *Melampsora medusae* f. sp. *tremuloides*

Melampsora medusae f. sp. *tremuloides* (*Mmt*) was isolated from naturally infected *Populus tremuloides* leaves collected in Québec City. Urediniospores were scrapped with a stainless-steel single edge-dissecting needle, resuspended in sterile distilled water, and filtered on 100 μm BD Falcon cell strainer. The concentration of the urediniospores in the suspension was determined with an hemacytometer and adjusted to 10^5 conidia/mL. Leaves were detached from in vitro plantlets of wild-type and transgenic lines and placed onto a piece of Kimberley Clark Wypall L20 saturated with distilled water covering the surface of 100 mm Petri dishes. The urediniospores suspension was then spray-inoculated on the abaxial surface of the leaves with a siphon feed airbrush at an air pressure of 20 psi. Observation was performed 15 days post inoculation by counting *Mmt* uredinia present on the poplar leaves.

Effector in silico analyses

SignalP (https://services.healthtech.dtu.dk/services/SignalP-6.0/) was used to predict the signal peptide of the *Mlp* candidate effectors. Subcellular localization for the selected CSEPs was predicted using Localizer and WolfPSORT (https://wolfpsort.hgc.jp/) (Sperschneider et al. 2017), while nuclear localization signal (NLS) was predicted with NLStradamus (ht

Fig. 1. Mlp72983 and Mlp52166 are two similar CSEPs from *Mlp*. (A and B) Schematic representation of Mlp72983 and Mlp52166 proteins (in grey) indicating signal peptides and nuclear localization signal in the native proteins, and the localization of the GFP (in green) in the mature fusion proteins (without signal peptide). Host expression specificity is denoted by the larch tree (A) and poplar tree (B). (C) Full length amino acid alignment of Mlp72983 and Mlp52166 using Clustal Omega in R Studio. Identical amino acid sequence between both *Mlp* CSEPs in colored boxes.

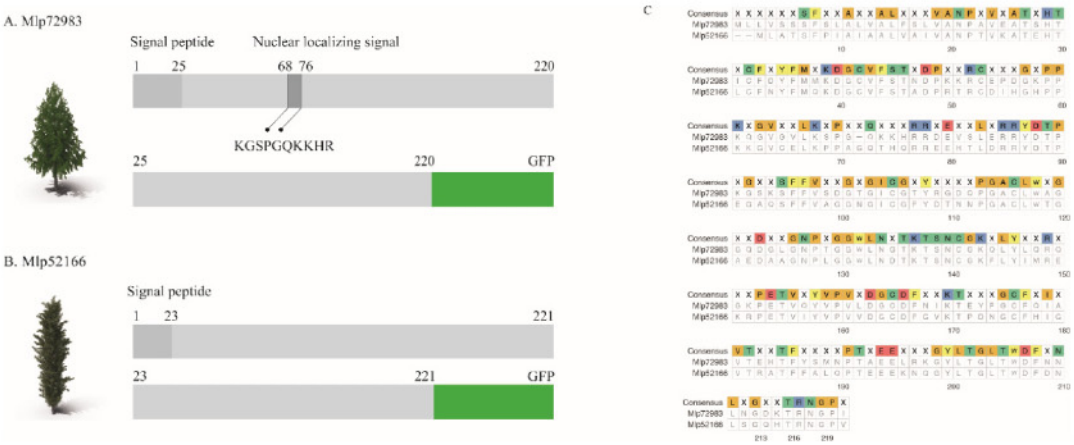

tp://www.moseslab.csb.utoronto.ca/NLStradamus/), presence of chloroplast transit peptide was assessed with TargetPv2.0 (https://services.healthtech.dtu.dk/services/TargetP-2.0/), and protein sequences were aligned using Clustal Omega (https://www.ebi.ac.uk/jdispatcher/) with R v4.3.1.

Results

Mlp72983 and Mlp52166 are two similar CSEPs from *Mlp*

Mlp72983 and Mlp52166 comprise a predicted signal peptide and 220 and 221 residues, respectively (Figs. 1A and 1B), and their sequences share 76.9% identity at the amino acid level (Fig. 1C). The analysis of the mature sequences (without signal peptide) with Localizer, TargetP, and WolfPSORT predicted neither chloroplast nor mitochondrial transit peptides (Table S3). Unlike Mlp52166, Mlp72983 carries an eight amino-acid long monopartite NLS (amino acids 68–76). To elucidate the distinctions between these homologous CSEPs, we first assessed their localization *in planta*.

In *Arabidopsis* cells, Mlp72983 displays a cell type-specific localization, whereas Mlp52166 accumulates in the nucleus and the cytosol

We assessed the localization of each CSEP in stable *A. thaliana* transgenic lines. In epidermal cells, the GFP control plant displays nucleocytosolic localization (Fig. 2A). Mlp72983-GFP shows cell type-specific accumulation detected exclusively in the chloroplast of the guard cells (Fig. 2B). Interestingly, Mlp72983-GFP fluorescence was detected in the chloroplasts of guard cells, but the signal was absent in the pavement cell. Surprisingly, Mlp72983-GFP signal was absent in pavement cells and only present in guard cells. Moreover, we observed Mlp72983-GFP signal in the nucleus of the spongy mesophyll cells (Fig. 2C). In contrast, transgenics expressing Mlp52166-GFP showed a fluorescent signal in the nucleus and the cytosol in the abaxial epidermal layer (Fig. 2D) and strictly to the nucleus of the spongy mesophyll cells (Fig. 2E). We detected no phenotypical difference between the *Arabidopsis* transgenics overexpressing Mlp72983-GFP or Mlp52166-GFP, and the control line (Col-0-GFP) (Supplementary Fig. 3). Because we observed the accumulation of Mlp72983 in chloroplasts, we investigated whether it affected the activity of Photosystem II in the *Arabidopsis* transgenics. We measured the ratio of maximum chlorophyll fluorescence yield (*Fv*/*Fm*) that indicates the photosystem activity in dark relaxed state. In both lines of *Arabidopsis* transgenics overexpressing Mlp72983, *Fv*/*Fm* showed similar photosystem activity compared to the control (Col-0-GFP) (Fig. S4). Based on these results, we concluded that despite their amino acid similarities, Mlp72983 and Mlp52166 have distinct subcellar localization patterns. More specifically, Mlp72983 has a cell type-specific localization and its chloroplastic localization did not perturb global photosynthetic activity in *Arabidopsis* plants.

In poplar cells, Mlp72983 and Mlp52166 localize as in *Arabidopsis*

We also assessed the subcellular accumulation pattern of Mlp72983 and Mlp52166 in poplar transgenics. As in *Arabidopsis*, the poplar-GFP control, here referred to as GFP, showed the expected fluorescence in the cytosol and nuclei (Fig. 3A). Figure 3B shows that Mlp72983-GFP accumulates specifically in the chloroplasts of guard cells. In the spongy mesophyll layer, fluorescence of Mlp72983-GFP colocalized with DAPI in the nuclei (Fig. 3C). In the epidermis, Mlp52166 showed nucleocytosolic localization as observed in *A. thaliana* (Fig. 3D), and colocalized with DAPI in the nuclei of the spongy mesophyll layer in poplar leaves (Fig. 3E). While performing the assessment of poplar

Fig. 2. Mlp72983 displays a cell type-specific localization, whereas Mlp52166 accumulates in nucleus and cytosol in Arabidopsis transgenics. Confocal images (A) Col-0 expressing GFP (used as control). (B) Mlp72983 fused with GFP in abaxial epidermal layer. (C) Spongy mesophyll layers showing fluorescence of Mlp72983. (D) Mlp52166 fused with GFP in epidermal layer. (E) Accumulation of Mlp52166-GFP fusion. Green fluorescent protein (green panel), chlorophyll autofluorescence (blue panel), DAPI (blue panel), merge of panels, fluorescence intensity of the overlap of fluorophores shown in the panels (right). Scale—10 μm.

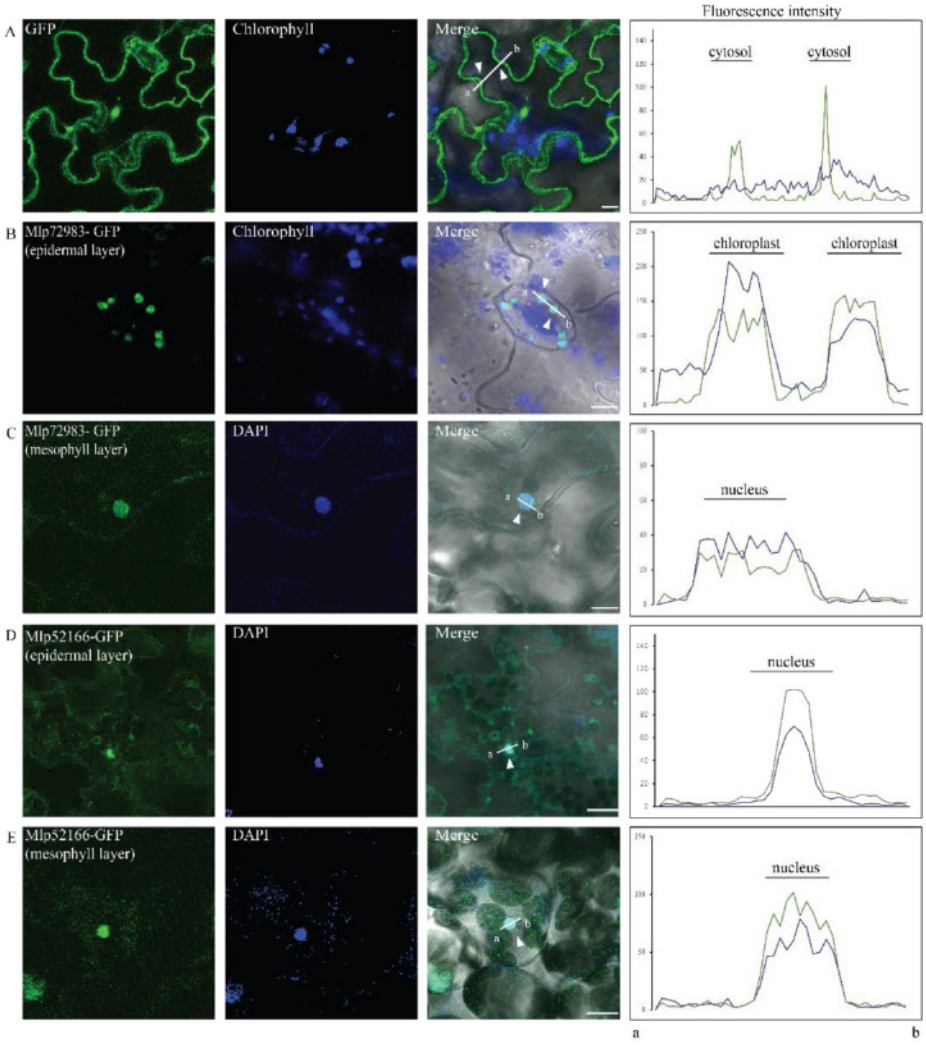

transgenics, we did not observe morphological differences with wild type (Fig. S5A). To rule out that the nucleocytosolic localization of Mlp52166-GFP was not a cleavage artifact, we performed a Western blot of the four transgenic lines. Mlp52166-GFP was detected at the expected molecular weight (48 KDa) in both lines, while Mlp72983-GFP was below the detection threshold in P1_LINE1_729 but detected at the appropriate molecular weight (48 KDa) in P1_LINE3_729 (Fig. S5B). We concluded that Mlp72983 has cell type-specific accumulation where it is restricted to guard cells in the epidermis, more precisely in the chloroplasts of guard cells, and the nucleus of spongy mesophyll layers. For its part, Mlp52166 shows a nucleocytosolic localization in epidermal layer and is strictly nuclear in spongy mesophyll layers. This localization is identical as observed in independent *Arabidopsis* transgenics.

Mlp72983 and Mlp52166 deregulated sets of genes in *Arabidopsis* and poplar transgenics

Given that a previous study reported massive gene deregulation of plant immunity genes in *Arabidopsis* transgenics expressing Mlp72983 (Dos Santos et al. 2021), we further investigated the impact of Mlp72983 and Mlp52166 on gene expression in both *Arabidopsis* and poplar. Two transgenic lines for each CSEP, in both *Arabidopsis* and poplar, were used for transcriptomic analysis. We compared transgenic lines overexpressing *Mlp* CSEP against GFP expressing control lines; the genes with log2 fold change ≥ 2 and adjusted p value < 0.01 were considered deregulated. In poplar, we found 7793 differentially expressed genes (DEGs), whereas *Arabidopsis* showed 2131 genes deregulated by either *Mlp* CSEP (Fig. 4A). Plants expressing Mlp72983-GFP showed 539 and 689 downregulated

Fig. 3. Poplar transgenics showed identical localization of the two *Mlp* CSEPs as observed in *Arabidopsis* transgenics. (A) Poplar 717-1B4-GFP (control). (B) Mlp72983-GFP in the epidermis (the lower line was used for colocalization). (C) Spongy mesophyll layer showing fluorescence of Mlp72983-GFP. (D) Mlp52166-GFP in epidermal layer. (E) Accumulation of Mlp52166-GFP fusion in mesophyll. Green fluorescent protein (green panel), chlorophyll autofluorescence (blue panel), DAPI (blue panel), merge of panels, fluorescence intensity (right). Scale—10 μm.

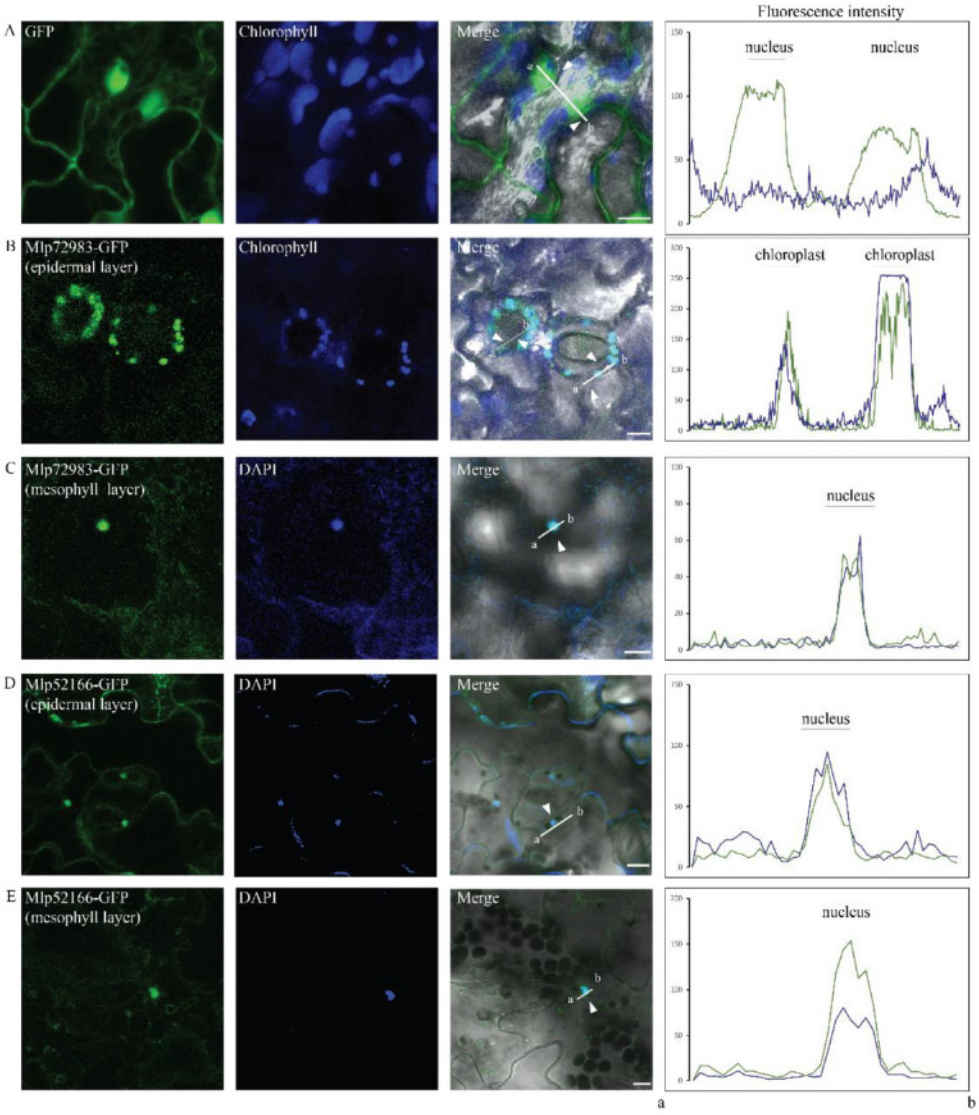

genes in *Arabidopsis* and poplar transgenics, respectively. On the other hand, Mlp52166 downregulated 825 genes in poplar and 231 in *Arabidopsis* transgenic lines. The list of common deregulated genes by *Mlp* CSEPs in each species can be found in Table S4.

We further determined the biological processes affected by Mlp72983 and Mlp52166 in the transgenic plants through GO term enrichment analysis. Figure 4B shows that, in poplar, the sets of genes downregulated by the two CSEPs are mostly enriched in processes such as DNA replication initiation, ATP biosynthesis, lignin catabolism, and signaling of mitotic spindle assembly. On the other hand, in *Arabidopsis*, the downregulated genes are related to response against biotic stress, signal transduction, negative regulation of innate immune response, and lipid biosynthesis.

To compare the deregulated genes between the two homologous CSEPs and between *Arabidopsis* and poplar, we used the *Ensembl* annotations for *A. thaliana* and *Populus trichocarpa* to find the orthologs between the two species. In the Venn diagram (Fig. 4C), the ellipses indicate that the genes deregulated in each species and by each CSEP, where upregulated and downregulated genes are indicated, respectively, in red and blue. Interestingly, we found that both CSEPs downregulate four common genes in each transgenics, namely AT3G53650 and Potri.010G231300 (histone superfamily), AT2G04050 and Potri.017G120400 (multidrug and toxic compound extrusion), as well as two genes with similar functions: AT3G47350, Potri.008G030600, and AT3G47360 and Potri.016G048800 (hydroxysteroid dehydrogenase). In conclusion, the two studied candidate effectors deregulate very

Fig. 4. Mlp72983 and Mlp52166 deregulated common sets of genes in *Arabidopsis* and poplar transgenics. (A) Heatmap of differential expressed genes (DEGs) in stable transgenics expressing *Mlp* CSEPs. The total number of deregulated genes in each plant species are indicated at the top of the heatmap. Up- and downregulated genes are represented, respectively, in red and blue (on the right), while two independent transgenics lines from each *Mlp* CSEPs are annotated on the left. (B) Cytoscape representation of downregulated genes involved in biological process in both the transgenics expressing *Mlp* CSEPs. (C) Identification of common homologous deregulated genes in both the stable transgenic species by Mlp72983 and Mlp52166 shown in Venn diagram. Here, upregulated (red) and downregulated (blue) genes are written as found in *Arabidopsis* followed by ortholog in poplar, respectively.

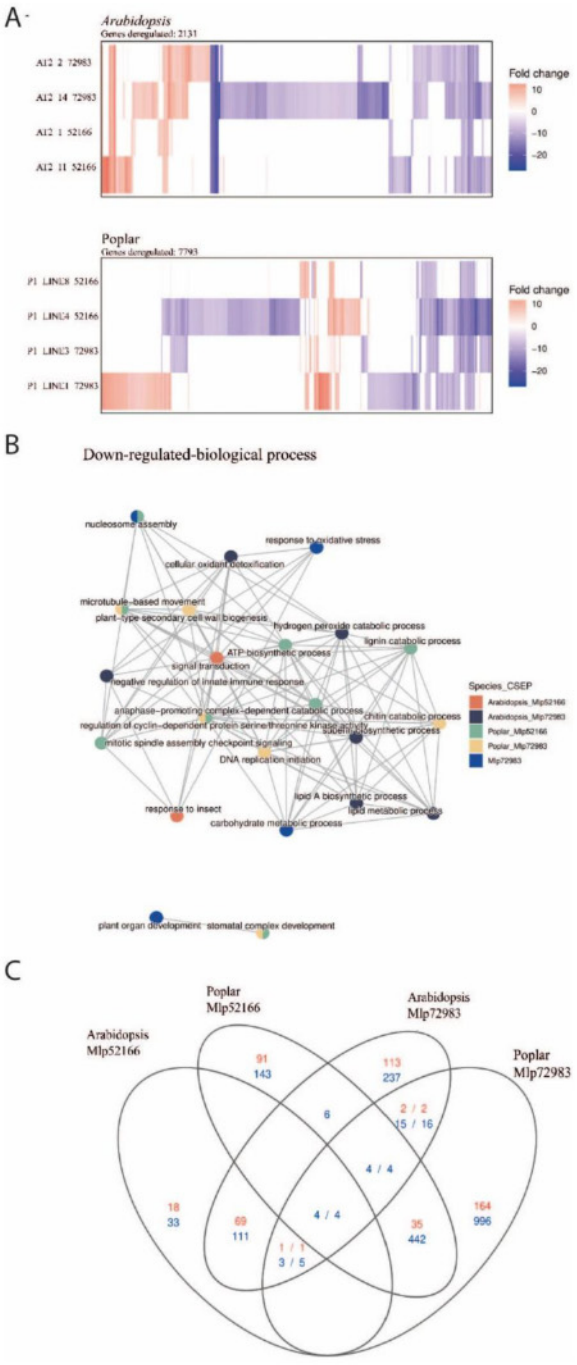

different gene sets while also deregulating a handful of common genes.

Poplar transgenics overexpressing *Mlp* CSEPs have normal infection levels of *Melampsora medusae* f. Sp. *Tremuloides*

As effectors commonly assist pathogen infection, we investigated the impact of *Mlp* CSEPs overexpression on poplar susceptibility to a rust fungal infection. As the poplar variety amenable to transformation (INRA clone 717-1B4) cannot be infected by *Mlp*, we infected our transgenic lines with *Melampsora medusae* f. sp. *tremuloides* (*Mmt*), a close relative of *Mlp*. In the infection assay, poplar transgenic leaves were inoculated with *Mmt* urediniospores and uredia was quantified 15 days later. A representative image of the *Mmt* pustules present on the poplar leaves is shown in Fig. 5A. Quantitative analysis indicated that *in planta* overexpression of the CSEPs did not promote the growth of *Mmt* on transgenic poplar (Fig. 5B).

Discussion

In this study, we have demonstrated that *Mlp* CSEPs have cell type-specific accumulation *in planta* and deregulates several genes in stable transgenics, including four common downregulated genes in two stable transgenic of the two studied CSEPs.

Our study revealed that Mlp72983 strictly targets the chloroplast of the guard cells in the epidermal pavement cells, and the nucleus of the spongy mesophyll cells in both poplar and *Arabidopsis* transgenics (Figs. 2 and 3). The cell type-specific accumulation suggests a dual role, one in the chloroplast of the guard cell and one in the mesophyll cells. Additionally, the nuclear localization of Mlp72983 is supported by the *in silico* prediction of an NLS in its amino acid sequence (Fig. 1A). The fact that Mlp72983 localizes to the chloroplasts (that has its own DNA) along with the nucleus in the studied stable transgenics could be due to the possible interaction of this candidate effector with DNA or DNA-binding proteins *in planta*. We also observed that Mlp72983 did not impair the photosynthetic activity of *Arabidopsis* transgenics (Supplementary Fig. 4). However, we cannot exclude an impact on photosynthesis of the guard cells since it could have been masked by the photosynthesis of the mesophyll cells.

The bioinformatic prediction tools did not identify compartment-specific addressing motifs in Mlp52166 (Figs. 2C and 3C). Mlp52166 also displayed cell type-specific localization as it is nucleocytosolic in pavement cells and nuclear in mesophyll cells. Interestingly, AvrB and AvrPto were shown to accumulate at different levels in diverse cell types and in a temporally regulated manner (Henry et al. 2017). In *Mlp*, the temporal regulation of effectors has been demonstrated previously (Hacquard et al. 2010). Although laser-dissection assisted transcriptomic had yielded insight the cell type-specific accumulation of effector's transcript (Hacquard et al. 2010), our results bring another level of understanding into the protein accumulation and cell-specific subcellular localization of *Mlp* effectors.

Fig. 5. *Mlp* CSEPs have normal infection levels to *Melampsora medusae* f. sp. *tremuloides* (*Mmt*). (A) Representation of presence of *Mmt* pustules on poplar leaves expressing *Mlp* CSEPs (i) Poplar-GFP, (ii) Poplar-717–1B4, (iii) P1_LINE1_72983, (iv) P1_LINE3_72983, (v) P1_Line4_52166, and (vi) P1_LINE8_52166. (B) Number of *Mmt* rust pustules per cm^2 on poplar leaves at 15 days post inoculation. No statistical differences were found using ANOVA analysis.

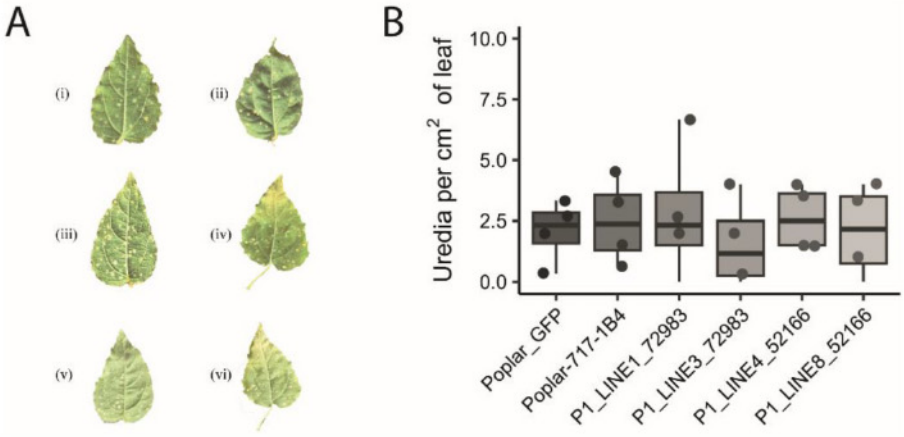

The two studied *Mlp* CSEPs deregulated 7793 genes in poplar and 2131 genes in *Arabidopsis* transgenics. The difference in the total number of deregulated genes between the species is likely due to the genome size and gene number. Indeed, *P. trichocharpa* has almost 520 megabases of DNA and 45 000 annotated coding genes, compared with the 125 megabases and 25 000 annotated genes of *A. thaliana* (Meinke et al. 1998; Tuskan et al. 2004). As Mlp52166 is expected to exhibit activity in poplar but not necessarily in *Arabidopsis,* which is not a host for the rust, this may contribute to the larger number of deregulated genes in poplar. Simply put, the effector may have more success exerting its full activity in its natural host. Among the genes downregulated by Mlp72983 in poplar, the top enrichment of the GO terms are in DNA replication initiation, plant-type secondary cell wall biogenesis, microtubule-based movement, chitin catabolic process, and regulation of cyclin-dependent serine/threonine kinase activity (Fig. 4B). The deregulated genes enrichment in GO categories of biological process in both *Arabidopsis* and poplar is shown in Figs. S6A and S6B. Interestingly, we identified the gene ID of four genes commonly downregulated among all the transgenic lines in both species (Fig. 4C). They encode for a histone superfamily protein, two hydroxysteroid dehydrogenases, and a multidrug and toxic compound extrusion protein. This common deregulation of genes may indicate that these *Mlp* CSEPs have similar indirect targets in the plant cells and, hence, modulate the expression of similar genes in both *Arabidopsis* and poplar species.

We did not detect enhanced susceptibility of *Populus* expressing either CSEPs to the poplar leaf rust fungus *Melampsora medusae* f. sp. *tremuloides*. This result differs from Germain et al. (2018), where stable *Arabidopsis* transgenics overexpressing Mlp72983 were more susceptible to oomycete infection. The lack of enhanced *Mmt* susceptibility caused by these two *Mlp* CSEPs could be due to a lack of sensitivity in the response variable we measured (uredia count), the requirement for a helper effector or the fact that *Mmt* already expresses candidate effector homologous to Mlp52166 and Mlp72983. The lack of genetic tools prevents the knock down or knock out of these candidate effectors in the *Mlp* or *Mmt* pathogen, which limits the assessment of their role during infection.

Taken together, our results show that these two *Mlp* CSEPs, despite having relatively high amino acid similarity, have different localization patterns. Interestingly, despite the extensive use of effector-GFP fusion in effectoromics experiments, cell-type specific subcellular accumulation has not been extensively reported. This may be due to the extensive use of the *N. benthamiana* transient expression system in which almost exclusively the pavement cells are imaged and guard cells do not express the transgene. Our results suggest that using stable transgenic provides an added value over transient expression for a better understanding of effector mechanistic.

Acknowledgements

The project was funded by Natural Sciences and Engineering Research Council of Canada Discovery Grant to HG. The project in HG's laboratory was also funded by an institutional research chair and a Canada Research Chair held by HG. SG has received funding from Bourse du programme d'appui à l'internationalisation de la recherche (PAIR Grant), Mobility Grant by Université du Québec à Trois-Rivières and Centre de recherche interinstitutionnel en sciences du végétal (SEVE). We are thankful to Guy Samson for his assistance with the photosynthetic measurements. This research was enabled in part by support provided by Calcul Québec (https://www.calculquebec.ca/) and the Digital Research Alliance of Canada (alliancecan.ca).

Article information

History dates

Received: 3 September 2024
Accepted: 28 January 2025
Accepted manuscript online: 5 February 2025
Version of record online: 13 March 2025

Data availability

Transcriptomic data shown in the study (raw reads and count matrices) can be accessed in NCBI with Bioproject PRJNA1072118. The scripts used in the transcriptomics analysis are available at the Github repository: https://github.com/SnehiG/Snehi_paper_2024/tree/patch-1/scripts.

Author information

Author ORCIDs

Hugo Germain https://orcid.org/0000-0002-7046-6194

Author contributions

Conceptualization: SG, AS, PT, BP, HG
Data curation: HG
Formal analysis: SG, KCGdS, HG
Funding acquisition: HG
Investigation: SG, BP, HG
Methodology: SG, KCGdS, MBP, CL, PT, HG
Project administration: HG
Resources: HG
Supervision: BP, HG
Writing – original draft: SG
Writing – review & editing: SG, MBP, CL, AS, PT, BP, HG

Competing interests

The authors declare no conflict of interest.

Supplementary material

Supplementary data are available with the article at https://doi.org/10.1139/cjfr-2024-0225.

References

Abdollahi, F., Alebrahim, M.T., Ngov, C., Lallemand, E., Zheng, Y., Villette, C., et al. 2021. Innate promiscuity of the CYP706 family of P450 enzymes provides a suitable context for the evolution of dinitroaniline resistance in weed. New Phytol. **229**(6): 3253–3268. doi:10.1111/nph.17126. PMID: 33253456.

Ahmed, M.B., Santos, K.C.G.d., Sanchez, I.B., Petre, B., Lorrain, C., Plourde, M.B., et al. 2018. A rust fungal effector binds plant DNA and modulates transcription. Sci. Rep. **8**(1): 14718. doi:10.1038/s41598-018-32825-0. PMID: 30283062.

Alfano, J.R. 2009. Roadmap for future research on plant pathogen effectors. Mol. Plant Pathol. **10**(6): 805–813. doi:10.1111/j.1364-3703.2009.00588.x. PMID: 19849786.

Andac, A., Ozketen, A.C., Dagvadorj, B., and Akkaya, M.S. 2020. An effector of *Puccinia striiformis* f. sp. tritici targets chloroplasts with a novel and robust targeting signal. Eur. J. Plant Pathol. **157**: 751–765. doi:10.1007/s10658-020-02033-6.

Carlson, M. 2019. org.At.tair.db: Genome wide annotation for Arabidopsis. p. R package.

Chen, S. 2023. Ultrafast one-pass FASTQ data preprocessing, quality control, and deduplication using fastp. iMeta, **2**. doi:10.1002/imt2.107.

Chen, S., Zhou, Y., Chen, Y., and Gu, J. 2018. fastp: an ultra-fast all-in-one FASTQ preprocessor. Bioinformatics, **34**(17): i884–i890. doi:10.1093/bioinformatics/bty560. PMID: 30423086.

Csardi, G., and Nepusz, T. 2006. The igraph software package for complex network research. InterJ. Complex Syst. **1695**(5): 1–9.

Csárdi, G., Nepusz, T., Traag, V., Horvát, S., Zanini, F., Noom, D., and Müller, K. 2023. igraph: network analysis and visualization in R. R package version 1.5. 1. doi:10.5281/zenodo.7682609.

Dean, R., Van Kan, J.A., Pretorius, Z.A., Hammond-Kosack, K.E., Di Pietro, A., Spanu, P.D., et al. 2012. The top 10 fungal pathogens in molecular plant pathology. Mol. Plant Pathol. **13**(4): 414–430. doi:10.1111/j.1364-3703.2011.00783.x. PMID: 22471698.

Delannoy, E., Batardiere, B., Pateyron, S., Soubigou-Taconnat, L., Chiquet, J., Colcombet, J., and Lang, J. 2023. Cell specialization and coordination in *Arabidopsis* leaves upon pathogenic attack revealed by scRNA-seq. Plant Commun. **4**(5). doi:10.1016/j.xplc.2023.100676. PMID: 37644724.

Dos Santos, K.C.G., Desgagné-Penix, I., and Germain, H. 2020. Custom selected reference genes outperform pre-defined reference genes in transcriptomic analysis. BMC Genom. **21**: 1–9. doi:10.1186/s12864-019-6426-2.

Dos Santos, K.C.G., Pelletier, G., Séguin, A., Guillemette, F., Hawkes, J., Desgagné-Penix, I., and Germain, H. 2021. Unrelated fungal rust candidate effectors act on overlapping plant functions. Microorganisms, **9**(5): 996. doi:10.3390/microorganisms9050996. PMID: 34063040.

Duplessis, S., Cuomo, C.A., Lin, Y.-C., Aerts, A., Tisserant, E., Veneault-Fourrey, C., et al. 2011. Obligate biotrophy features unraveled by the genomic analysis of rust fungi. Proc. Natl. Acad. Sci. USA, **108**(22): 9166–9171. doi:10.1073/pnas.1019315108.

Duplessis, S., Major, I., Martin, F., and Séguin, A. 2009. Poplar and pathogen interactions: insights from populus genome-wide analyses of resistance and defense gene families and gene expression profiling. Crit. Rev. Plant Sci. **28**(5): 309–334. doi:10.1080/07352680903241063.

Durinck, S., Spellman, P.T., Birney, E., and Huber, W. 2009. Mapping identifiers for the integration of genomic datasets with the R/bioconductor package biomaRt. Nat. Protoc. **4**(8): 1184–1191. doi:10.1038/nprot.2009.97. PMID: 19617889.

Frey, P., Hecker, A., Rouhier, N., and Duplessis, S. 2011. The poplar–poplar rust interaction: insights from genomics and transcriptomics. J. Pathogens. PMID: 22567338.

George, N.I., and Chang, C.-W. 2014. DAFS: a data-adaptive flag method for RNA-sequencing data to differentiate genes with low and high expression. BMC Bioinform. **15**: 1–11. doi:10.1186/1471-2105-15-92. PMID: 24383880.

Germain, H., Joly, D.L., Mireault, C., Plourde, M.B., Letanneur, C., Stewart, D., et al. 2018. Infection assays in *Arabidopsis* reveal candidate effectors from the poplar rust fungus that promote susceptibility to bacteria and oomycete pathogens. Mol. Plant Pathol. **19**(1): 191–200. doi:10.1111/mpp.12514. PMID: 27868319.

Hacquard, S., Delaruelle, C., Legué, V., Tisserant, E., Kohler, A., Frey, P., et al. 2010. Laser capture microdissection of uredinia formed by *Melampsora larici-populina* revealed a transcriptional switch between biotrophy and sporulation. Mol. Plant-Microbe Interact. **23**(10): 1275–1286. doi:10.1094/MPMI-05-10-0111. PMID: 20831407.

Hacquard, S., Joly, D.L., Lin, Y.-C., Tisserant, E., Feau, N., Delaruelle, C., et al. 2012. A comprehensive analysis of genes encoding small secreted proteins identifies candidate effectors in *Melampsora larici-populina* (poplar leaf rust). Mol. Plant-Microbe Interact. **25**(3): 279–293. doi:10.1094/MPMI-09-11-0238. PMID: 22046958.

Henry, E., Toruño, T.Y., Jauneau, A., Deslandes, L., and Coaker, G. 2017. Direct and indirect visualization of bacterial effector delivery into diverse plant cell types during infection. Plant Cell **29**(7): 1555–1570. doi:10.1105/tpc.17.00027. PMID: 28600390.

Joly, D.L., Feau, N., Tanguay, P., and Hamelin, R.C. 2010. Comparative analysis of secreted protein evolution using expressed sequence tags from four poplar leaf rusts (*Melampsora* spp.). BMC Genom. **11**: 1–16. doi:10.1186/1471-2164-11-422. PMID: 20044946.

Lawrence, M., Huber, W., Pagès, H., Aboyoun, P., Carlson, M., Gentleman, R., et al. 2013. Software for computing and annotating genomic

ranges. PLoS Comput. Biol. **9**(8): e1003118. doi:10.1371/journal.pcbi.1003118. PMID: 23950696.

Leple, J.C., Brasileiro, A.C.M., Michel, M.F., Delmotte, F., and Jouanin, L. 1992. Transgenic poplars: expression of chimeric genes using four different constructs. Plant Cell Rep. **11**: 137–141. doi:10.1007/BF00232166. PMID: 24213546.

Letanneur, C., Brisson, A., Bisaillon, M., Devèze, T., Plourde, M.B., Schattat, M., et al. 2024. Host-specific and homologous pairs of *Melampsora larici-populina* effectors unveil novel *Nicotiana benthamiana* stromule induction factors. Mol. Plant-Microbe Interact. **37**(3): 277–289. doi:10.1094/MPMI-09-23-0148-FI. PMID: 38148279.

Lorrain, C., Marchal, C., Hacquard, S., Delaruelle, C., Pétrowski, J., Petre, B., et al. 2018b. The rust fungus *Melampsora larici-populina* expresses a conserved genetic program and distinct sets of secreted protein genes during infection of its two host plants, larch and poplar. Mol. Plant-Microbe Interact. **31**(7): 695–706. doi:10.1094/MPMI-12-17-0319-R. PMID: 29336199.

Lorrain, C., Petre, B., and Duplessis, S. 2018a. Show me the way: rust effector targets in heterologous plant systems. Curr. Opin. Microbiol. **46**: 19–25. doi:10.1016/j.mib.2018.01.016. PMID: 29454191.

Love, M.I., Huber, W., and Anders, S. 2014. Moderated estimation of fold change and dispersion for RNA-seq data with DESeq2. Genome Biol. **15**(12): 1–21. doi:10.1186/s13059-014-0550-8.

Meinke, D.W., Cherry, J.M., Dean, C., Rounsley, S.D., and Koornneef, M. 1998. *Arabidopsis thaliana*: a model plant for genome analysis. Science, **282**(5389): 662–682. doi:10.1126/science.282.5389.662. PMID: 9784120.

Mireault, C., Paris, L.-E., and Germain, H. 2014. Enhancement of the Arabidopsis floral dip method with XIAMETER OFX-0309 as alternative to Silwet L-77 surfactant. Botany, **92**(7): 523–525. doi:10.1139/cjb-2014-0048.

Morgan, M., Pages, H., Obenchain, V., and Hayden, N. 2017. Binary alignment (BAM), FASTA, variant call (BCF), and tabix file import. R Packag. version 1(0).

Pedersen, T.L. 2020. ggraph: an implementation of grammar of graphics for graphs and networks. R package p. 0.9000.

Persoons, A., Hayden, K.J., Fabre, B., Frey, P., De Mita, S., Tellier, A., and Halkett, F. 2017. The escalatory Red Queen: population extinction and replacement following arms race dynamics in poplar rust. Mol. Ecol. **26**(7): 1902–1918. doi:10.1111/mec.13980. PMID: 28012228.

Petre, B., and Duplessis, S. 2022. A decade after the first Pucciniales genomes: a bibliometric snapshot of (post) genomics studies in three model rust fungi. Front. Microbiol. **13**: 989580. doi:10.3389/fmicb.2022.989580. PMID: 36187960.

Petre, B., Lorrain, C., Saunders, D.G., Win, J., Sklenar, J., Duplessis, S., and Kamoun, S. 2016. Rust fungal effectors mimic host transit peptides to translocate into chloroplasts. Cell. Microbiol. **18**(4): 453–465. doi:10.1111/cmi.12530. PMID: 26426202.

Petre, B., Saunders, D.G., Sklenar, J., Lorrain, C., Win, J., Duplessis, S., and Kamoun, S. 2015. Candidate effector proteins of the rust pathogen *Melampsora larici-populina* target diverse plant cell compartments. Mol. Plant-Microbe Interact. **28**(6): 689–700. doi:10.1094/MPMI-01-15-0003-R. PMID: 25650830.

Pinon, J., and Frey, P. 2005. Interactions between poplar clones and *Melampsora* populations and their implications for breeding for durable resistance. *In* Rust diseases of willow and poplar. CABI Publishing Wallingford UK. pp. 139–154.

Saunders, D.G., Win, J., Cano, L.M., Szabo, L.J., Kamoun, S., and Raffaele, S. 2012. Using hierarchical clustering of secreted protein families to classify and rank candidate effectors of rust fungi. PLoS ONE, **7**(1): e29847. doi:10.1371/journal.pone.0029847. PMID: 22238666.

Slowikowski, K. 2024. ggrepel: automatically position non-overlapping text labels with 'ggplot2'.

Sperschneider, J., Catanzariti, A.-M., DeBoer, K., Petre, B., Gardiner, D.M., Singh, K.B., Dodds, P.N., and Taylor, J.M. 2017. LOCALIZER: subcellular localization prediction of both plant and effector proteins in the plant cell. Sci. Rep. **7**(1): 44598.

Tang, B., Feng, L., Hulin, M.T., Ding, P., and Ma, W. 2023. Cell-type-specific responses to fungal infection in plants revealed by single-cell transcriptomics. Cell Host Microbe, **31**(10): 1732–1747. e1735.

Tuskan, G.A., DiFazio, S., and Teichmann, T. 2004. Poplar genomics is getting popular: the impact of the poplar genome project on tree research. Plant Biol. **6**(1): 2–4. doi:10.1055/s-2003-44715.

Vigneault, F., Lachance, D., Cloutier, M., Pelletier, G., Levasseur, C., and Séguin, A. 2007. Members of the plant NIMA-related kinases are involved in organ development and vascularization in poplar, *Arabidopsis* and rice. Plant J. **51**(4): 575–588. doi:10.1111/j.1365-313X.2007.03161.x.

Xhaard, C., Fabre, B., Andrieux, A., Gladieux, P., Barres, B., Frey, P., and Halkett, F. 2011. The genetic structure of the plant pathogenic fungus *Melampsora larici-populina* on its wild host is extensively impacted by host domestication. Mol. Ecol. **20**(13): 2739–2755. doi:10.1111/j.1365-294X.2011.05138.x.

Xu, Q., Tang, C., Wang, X., Sun, S., Zhao, J., Kang, Z., and Wang, X. 2019. An effector protein of the wheat stripe rust fungus targets chloroplasts and suppresses chloroplast function. Nat. Commun. **10**(1): 5571. doi:10.1038/s41467-019-13487-6.

Yu, G. 2020. Gene ontology semantic similarity analysis using GOSemSim. Stem Cell Transcriptional Networks: Methods and Protocols. pp. 207–215.

Yu, G., Li, F., Qin, Y., Bo, X., Wu, Y., and Wang, S. 2010. GOSemSim: an R package for measuring semantic similarity among GO terms and gene products. Bioinformatics, **26**(7): 976–978. doi:10.1093/bioinformatics/btq064.

Yu, G., Wang, L.-G., Han, Y., and He, Q.-Y. 2012. clusterProfiler: an R package for comparing biological themes among gene clusters. Omics, **16**(5): 284–287. doi:10.1089/omi.2011.0118.